

Local and regional processes drive distance decay in structure in a spatial multilayer plant-pollinator network

Agustin Vitali¹, Maya Goldstein¹, Matan Markfeld¹, and Shai Pilosof^{1,2,*}

¹Department of Life Sciences, Ben-Gurion University of the Negev, Beer-Sheva, Israel

²The Goldman Sonnenfeldt School of Sustainability and Climate Change, Ben-Gurion University of the Negev, Be'er Sheva, Israel

*Correspondence: pilos@bgu.ac.il

¹Equal contribution

Abstract

Understanding spatial variation in species distribution and community structure is at the core of biogeography and community ecology. Nevertheless, the effect of distance on metacommunity structure remains little studied. We use plant-pollinator network data from the Canary Islands to examine how plant-pollinator community structure changes across geographical distances at a regional scale and disentangle its underlying local and regional processes. We represent plant-pollinator communities as a metacommunity using a multilayer network. We quantified multilayer modularity to test for distance decay in structure across space. In multilayer modularity, the same species can belong to different modules in different layers, and modules can span layers. This enabled quantifying how similarity in module composition varied with distance between locations. We developed four null models, each controlling for a separate component of the multilayer network, to disentangle the role of species turnover, interaction rewiring, and local factors in driving distance decay in module similarity. We found a pattern of distance decay in structure, indicating that locations tended to share fewer modules with increasing distance. Species turnover (but not interaction rewiring) was the primary regional process triggering distance decay in structure. Local factors also played an essential role in determining the structure similarity of communities at a regional scale. These local differences could, in turn, influence regional processes occurring between locations. Finally, the extent to which species shared partners across locations did not affect distance decay in structure. Our work highlights the interplay between local and regional processes underlying biogeographic patterns. Our methodology provides a general framework for linking communities in space and testing different hypotheses regarding the factors generating spatial structure.

Introduction

Understanding spatial variation in species distribution and community structure is at the core of biogeography and community ecology. Across space, turnover of species and interactions occur due to variations in local environmental conditions, species traits, and ecological processes such as dispersal and the loss and gain of species interactions [1–4]. A well-documented phenomenon is distance decay—the decreasing similarity in species composition and interactions between two locations as the distance between them increases [5–9]. Distance decay is primarily driven by species turnover [9]. However, interaction turnover can also emerge when species rewire their interactions within the same species pool [7,9,10]. Together, species turnover and interaction rewiring alter the way species interact and their functional role across space [7,10–12], which, in turn, can affect the structure of local communities and the metacommunity. Understanding how community structure varies across space is necessary because structure ultimately affects community stability and function [13–15]. Nevertheless, the effect of geographical distance on community structure remains little studied [16].

Barriers to connectivity (e.g., rivers, mountain ridges) can also influence species turnover and interaction rewiring throughout space [17]. This phenomenon is similar to population genetics, where genetic differences between populations rise either due to barriers or isolation by distance [18]. In this paper, we focus on distance effects. Previous analyses of ecological networks found that similarity in species and interaction composition decrease across geographic distances [9,19]. However, distance decay in structure has been little studied [16]. Dallas & Poisot [16] did not find evidence for distance-decay in host-parasite network structure (based on node’s centrality and connectivity and distance among nodes), despite high species turnover across space. Nevertheless, that study considered each local community as an independent entity. Therefore, the properties of local networks were calculated independently. In contrast, in nature, communities are connected (e.g., by species dispersal), and share species. While such interdependence can be considered by analyzing a network that aggregates all species and interactions across localities (often termed the metaweb) [7], this approach ignores the spatial distribution of communities.

Here, we test for distance decay in the spatial structure of a metacommunity. We do so by linking local communities using a multilayer network approach, forming a *spatial multilayer network*. Multilayer networks are particularly adequate for investigating spatial effects on community structure because they contain two kinds of links [20]. Intralayer links encode species interactions within a community (e.g., pollination), while interlayer links describe variation across communities, capturing the effect of processes such as dispersal or species turnover. This approach allows uncovering hidden patterns and drivers that simultaneously shape structure at the local and regional scales. A recent study used a multilayer network to describe the meta-co-occurrence network in the rumen microbiome but did not consider distance [21].

We expand the concept of distance decay in species to that of distance decay in structure by exploring multilayer modularity. Modularity describes the extent to which the community is partitioned into groups of densely interacting species [22]. In turn, this structure can affect community stability [23]. At the local scale, modular structure arises from local factors, such as environmental conditions and habitat heterogeneity [24]. For example, species can adapt to exploit particular resources based on their availability, creating modules [25]. At the regional scale, modularity can arise due to geographic constraints (connectivity barriers) and distance decay in both species and interactions [24]. Therefore, *spatial modularity* is a signature emerging from both local and non-local processes. A previous study connected networks from four habitats and found that modules contained species from multiple habitats. However, this

study did not consider the location of the habitats and the interlayer links did not encode variation between local habitats [26].

Our goal is to test for *distance decay in structure* between communities using spatial modularity and disentangle the factors that generate this pattern. In multilayer networks, a module can span several local communities [20,26]. Therefore, distance decay in structure is a pattern in which the farther apart two local communities are, the less they share modules. We use data from local plant-pollinator networks in the Canary Islands, which we represent as a spatial multilayer network. This data set is particularly suitable because a previous study showed distance decay in species and interactions in this system [9]. Distance decay in species composition should strongly affect spatial modularity because if two locations are remote and do not share species, they are unlikely to share modules. We hypothesized that species turnover (H_1) and interaction rewiring across locations (H_2) drive distance decay in structure at the regional scale because both are processes that contribute to shape community structure [7,10]. We further hypothesized that factors occurring within each location (i.e., local factors) could affect structure distance decay (H_3) because they influence processes that favor modular structure, such as resource partitioning and coevolution [24,25]. Finally, we tested whether species' partner similarity across space triggers distance decay in modular structure (H_4) because it could increase the chances of sharing modular structures between locations. To test these alternative, yet not mutually exclusive, hypotheses we developed a set of four null models, which alter different components of the spatial multilayer network. These models allowed us to disentangle local vs. regional drivers in spatial modularity.

Methods

Study sites and data collection

We used data from Trøjelsgaard *et al.* [9]. The data were collected in six major volcanic-origin islands in the Atlantic Ocean (Canary Islands): El Hierro (27.804N, 17.895W), La Gomera (28.039N, 17.226W), Fuerteventura (28.564N, 13.891W), Gran Canaria (27.904N, 15.433W), Tenerife (28.353N, 16.912W) and Fasnía (28.222N, 16.417W), and one location on the mainland in Western Sahara (26.161N, 14.422W). As in the original publications, we too considered Fasnía and Tenerife as two separate islands due to their geological history [9,27]. We refer to the islands and mainland as 'locations'. Distances between locations ranged from 52 to 450 kilometers. In each location, pollinator-plant interactions were recorded at two sites (50 to 500 meters apart). Each site was sampled twice between January and March in 2010 and at each visit, pollinator-plant interactions were recorded by conducting four 15 min censuses per flowering plant. An interaction was recorded when the visitor touched the reproductive parts of the flower. A full description of the locations and sampling protocols is in Trøjelsgaard *et al.* [9].

Multilayer network construction

Our multilayer network represented a metacommunity (i.e., communities that are linked in the network), and contained four components [20]:

1. Seven layers representing six islands and the mainland. In the case of the Canary Islands, the decay pattern might be affected by distance or connectivity barriers within an island together with insularity effects (large distance between islands). Per the aim of this paper, we focused on insularity effects (including the mainland), rather than on local connectivity barriers within an island. Therefore, we aggregated data from any two adjacent sites within

an island or mainland by the union of interactions in both sites.

2. Two sets of nodes representing pollinator and plant species. Species can occur in more than one layer. Following standard terminology [20], we define plants and pollinator species as “physical nodes” and species-layer combinations as “state nodes”, indicating that the same species can have different ecological functions at different locations. For instance, a pollinator can contribute differently to pollination on different islands.
3. Intralayer directed weighted links representing pollination interactions within layers. An intralayer link from a pollinator species j to a plant species k in layer α was calculated as $w_{kj}^\alpha = f_{kj}/f_j$, where f_{kj} is the frequency of visits of j to k , and f_j is the total number of interactions of j in layer α . A link from a plant k to pollinator j was calculated similarly as $w_{jk}^\alpha = f_{kj}/f_k$, where f_k is the total number of visits plant k receives from all pollinators in layer α . This definition considers the asymmetric dependency between plants and pollinators [28].
4. Interlayer weighted links $w_i^{\alpha\beta}$ connecting any species i to itself between two layers when it occurs in both layers α and β and shares at least one partner. We calculated the value of interlayer links as the Jaccard similarity between the partners of i in the two layers. If species i shares all its partners between locations (high partner similarity), the value of the interlayer link is 1. Alternatively, the value approximates 0 when the interaction partners of i are dissimilar. Our interlayer link definition resonates with the concept of partner fidelity introduced in the original study [9]. It also captures spatial effects because there is a distance decay in species between islands [9].

Note that we did not define interlayer links based on distance because we use distance to test for distance decay. In addition, the definition of intralayer and interlayer links scales their weights between 0 and 1. This ensures that network properties, and particularly modularity, are not biased towards processes that occur within or between locations (Fig. S1) [20,26].

Distance decay in spatial modularity

We used modularity as the network property in which we quantify distance decay in structure. Modularity analysis detects groups of tightly interacting plant and pollinator species (modules). We chose modularity for two reasons. First, it is a well-described pattern in non-connected local communities [24]. Second, Unlike in monolayer modularity, in multilayer modularity, the same species can belong to different modules in different layers (i.e., islands/locations) [20,26,29]. In addition, modules can span layers. This unique feature of multilayer modularity is particularly useful for spatial analysis because it allows the detection of spatial patterns in species clustering. We quantified network partitioning to modules using the infomap algorithm [30,31] implemented in the `infomapecology` package in R [32,33]. Briefly, infomap minimizes the objective function L called the map equation using a modified Louvain algorithm. The optimal partition is that which minimizes the amount of information needed to describe the movement of a random walker across the network (lowest L). Infomap is particularly useful for analyzing spatial multilayer networks because it explicitly accounts for the multilayer network structure by considering both intralayer and interlayer links, and due to its computational efficiency [32].

We calculated similarity in module composition between locations using the Jaccard index. A value of 1 indicates that the two locations have exactly the same modules, while 0 indicates that the two locations do not share any module. We then used linear regression on distance matrices

(MRM) to test for distance decay in module similarity. That is, we used distance between pairs of locations and their similarity in module composition as the independent and response variables, respectively. MRM accounts for spatial autocorrelation in regression models because p-values and coefficients are obtained by randomization [34,35]. We performed the analyses with the stats, vegan, and ecodist packages in R [36,37].

Null models

Distance decay in spatial modularity could emerge from different drivers, such as turnover of species and interaction rewiring across locations, local factors occurring within locations, or simply be a result of random processes [1–3]. To disentangle these factors, we developed the following null models controlling for different components of the network.

- **H₁ - Species turnover (null model M_1 ; Fig. 1A).** To test if species turnover affects distance decay in module composition, we redistributed species randomly across locations. We shuffled plants (model M_1^P), pollinators (model M_1^A), or both (model M_1^{AP}) between layers. We randomly chose two physical nodes from different layers (e.g., two plants in model M_1^P) and switched their layers. For instance, when selecting nodes (x, α) and (y, β) for the switch, the outcome would be (x, β) and (y, α) after the exchange. We do not switch a species into a layer where it is already present; we performed 3,000 switches to ensure sufficient switches to meet this condition. This null model changes species labels and interlayer structure but not the intralayer structure.
- **H₂ - Interaction rewiring between layers (null model M_2 ; Fig. 1B).** We tested if interaction rewiring across locations affects distance decay in structure. To do this, we randomly shuffled interactions of each pair of species between all the layers in which they co-occur. For example, if a plant and a pollinator co-occurred in layers α and β but interacted only in layer α , they would still co-occur in the same layers but may interact in layer β after shuffling. Hence, null model M_2 shuffles intralayer links between layers while conserving species composition and the presence of interlayer links.
- **H₃ - Local factors (null model M_3 ; Fig. 1C).** To test if local factors within locations affect spatial modularity at the meta-community scale, we shuffled interactions within each layer. This is the common way of shuffling in monolayer bipartite networks. We kept the total sum of interactions constant and shuffled cells of each layer matrix (function `r00_samp` in the package `vegan` in R). After shuffling, we recalculated the directed intralayer links of each layer. This null model changes the intralayer structure but not the presence of interlayer links.
- **H₄ - The extent of partner similarity (null model M_4 ; Fig. 1D).** We tested if the extent to which species share partners across locations triggers distance decay in structure. We set the weight of the already existing interlayer links to a uniform value ranging from 0.1 to 1. Therefore, we disregard the existing number of shared partners and test if the *distribution* of interlayer link weights is important in determining spatial modularity. This null model conserves the intralayer structure and the presence of interlayer links.

For the null models M_1 , M_2 , and M_3 , we conducted 1,000 simulations and recalculated the distance decay in structure using linear regressions based on distance matrices, as we performed above for the empirical network. Then, we compared the degree of similarity in spatial modularity explained by distance (R^2 of the linear regression) in the empirical network to values

estimated from the shuffled networks. To do that, we calculated a p -value based on the proportion of R^2 values in the shuffled networks that are larger or smaller than the empirical value. Significant results indicate that the extent to which distance affects structure similarity in the empirical network is not random and depends on the factor considered in the null model. We did not perform these comparisons for null model M_4 , which we ran only once for each fixed value.

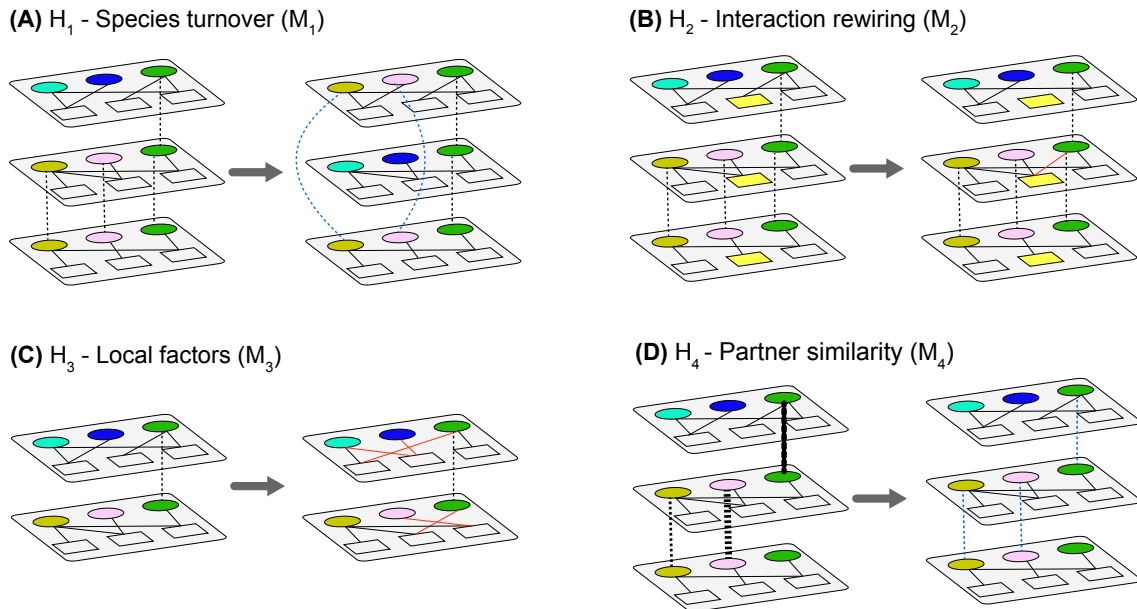


Fig. 1: Null models to test hypotheses for distance decay in spatial modularity. The networks depicted are bipartite multilayer networks that contain two sets of nodes (circles and squares), layers (polygons), intralayer links (solid lines), and interlayer links (dashed lines). For simplicity, we only colored one set of nodes (besides B) and did not differentiate the weight of links (besides D). **(A)** in M_1 we shuffled the occurrence of species between layers. In this example, we switched the brown and pink nodes for the cyan and blue nodes. These switches generated new interlayer links (dashed blue lines). **(B)** In M_2 we shuffle interactions between layers. In this example, the green and yellow nodes co-occur in all three layers but interact only in the upper layer. After the shuffling they now interact in the middle layer (red solid line). **(C)** In M_3 we shuffled intralayer links (red solid lines). This is the common way of shuffling in monolayer bipartite networks. **(D)** In M_4 we changed the weight of interlayer links (depicted by line width) to a uniform value from 0.1 to 1 (all blue dashed lines are the same width).

Results

The Canary Islands network shows distance decay in structure

We recorded 4,727 pollination links and 494 interlayer links connecting locations (Table S1, Fig. S1, Fig. S2A). 298 (60%) and 196 (40%) of interlayer links involved pollinator and plant species, respectively (Fig. S2B). The weight of interlayer links was, on average, higher for pollinator (0.41 ± 0.29 ; mean \pm SD) than for plant species (0.13 ± 0.08), which indicates that pollinators tend to share more partners between locations (Fig. S2B). The spatial network was partitioned into 42 modules. Modules varied in size, ranging from 2 to 53 species, with an average of 12 ± 14

species per module (Fig. S3, Fig. S4). Thirty one (73.8%) modules were found in more than one location, while 11 modules (26.2%) were confined to a single location (Fig. S5). The similarity in module composition between locations (Jaccard similarity index) was 0.32 ± 0.16 (Fig. 2). We recorded the maximum (0.56) and the minimum (0) structure similarity between the closest and the most distant locations respectively (Fig. 2).

We found a pattern of distance decay in spatial module similarity, as shown by the red line in all panels of Fig. 3 ($R^2 = 0.653$, $P < 0.001$, Table S2). Therefore, communities tended to share fewer modules with increasing distance.

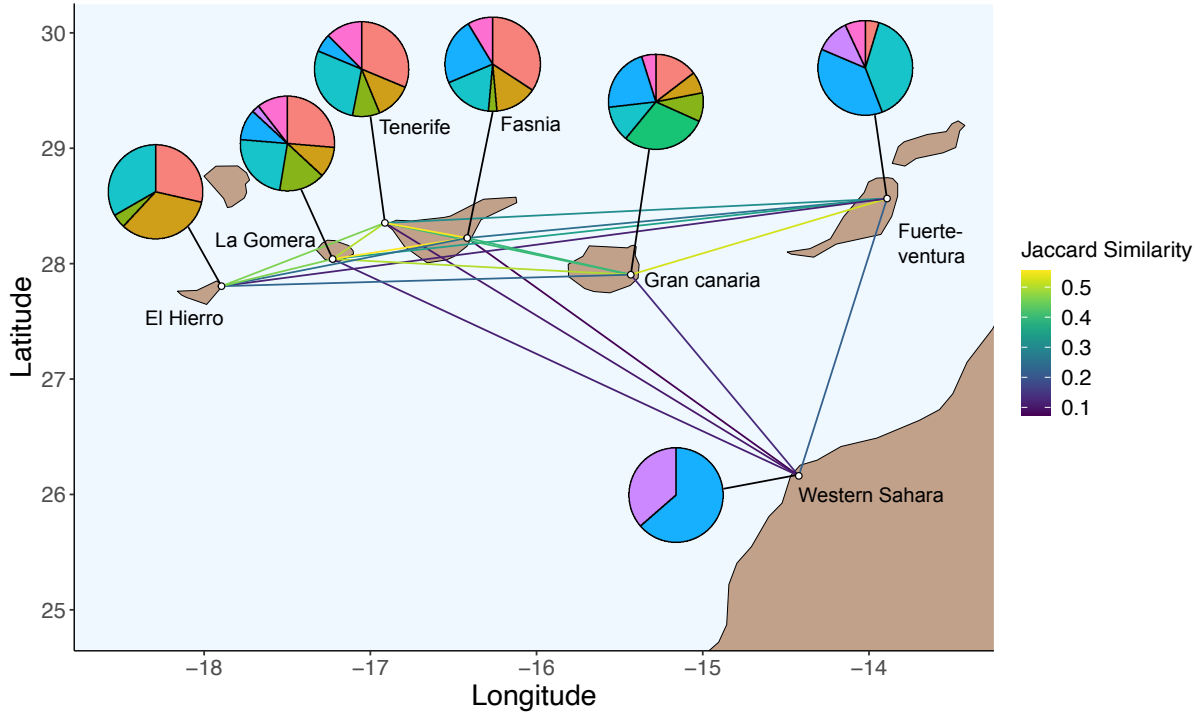


Fig. 2: Distance decay in modular structure. Each node in the network is a layer in the multilayer network. Edge color depicts the Jaccard similarity in module composition between layers. Pie charts indicate the spatial distribution of the eight largest modules. The color and size of portions within pie charts represent module ID and the proportion of species from that location in the module. For example, the red module is present in all islands (but not the mainland). See Fig. S2 for a detailed visualization of interlayer connectivity.

Species turnover and local factors drive distance decay in modularity

We used four null models to test alternative hypotheses that aim to disentangle the factors that generate distance decay in structure.

H₁ - Species turnover: Redistributing pollinator species alone, or the pollinators and plants, among locations eliminated the distance decay in module similarity ($R^2_{M_1^A} = 0.105$, $P = 0.267$; $R^2_{M_1^{AP}} = 0.169$, $P = 0.231$, purple and light blue lines in Fig. 3A, Table S2). While redistributing the plants alone still resulted in distance decay, it was weaker than the empirical observation ($R^2_{M_1^P} = 0.518$, $P < 0.01$, green line in Fig. 3A, Table S2). Consequently, the amount of variation in spatial module similarity explained by distance between locations was lower when we shuffled pollinators or both plants and pollinators than in the empirical network ($P < 0.005$, Fig. 4A). Therefore, the spatial distribution of pollinator species contributes to the distance decay in spatial modularity found in the empirical network.

H₂ - Interaction rewiring: Shuffling interactions between locations had little effect on distance decay in spatial modularity ($R_{M_2}^2 = 0.712$, $P < 0.001$, yellow line in Fig. 3B, Table S2). In addition, the amount of variation explained by the linear regressions did not change significantly after shuffling interactions between locations ($P = 0.84$, Fig. 4B).

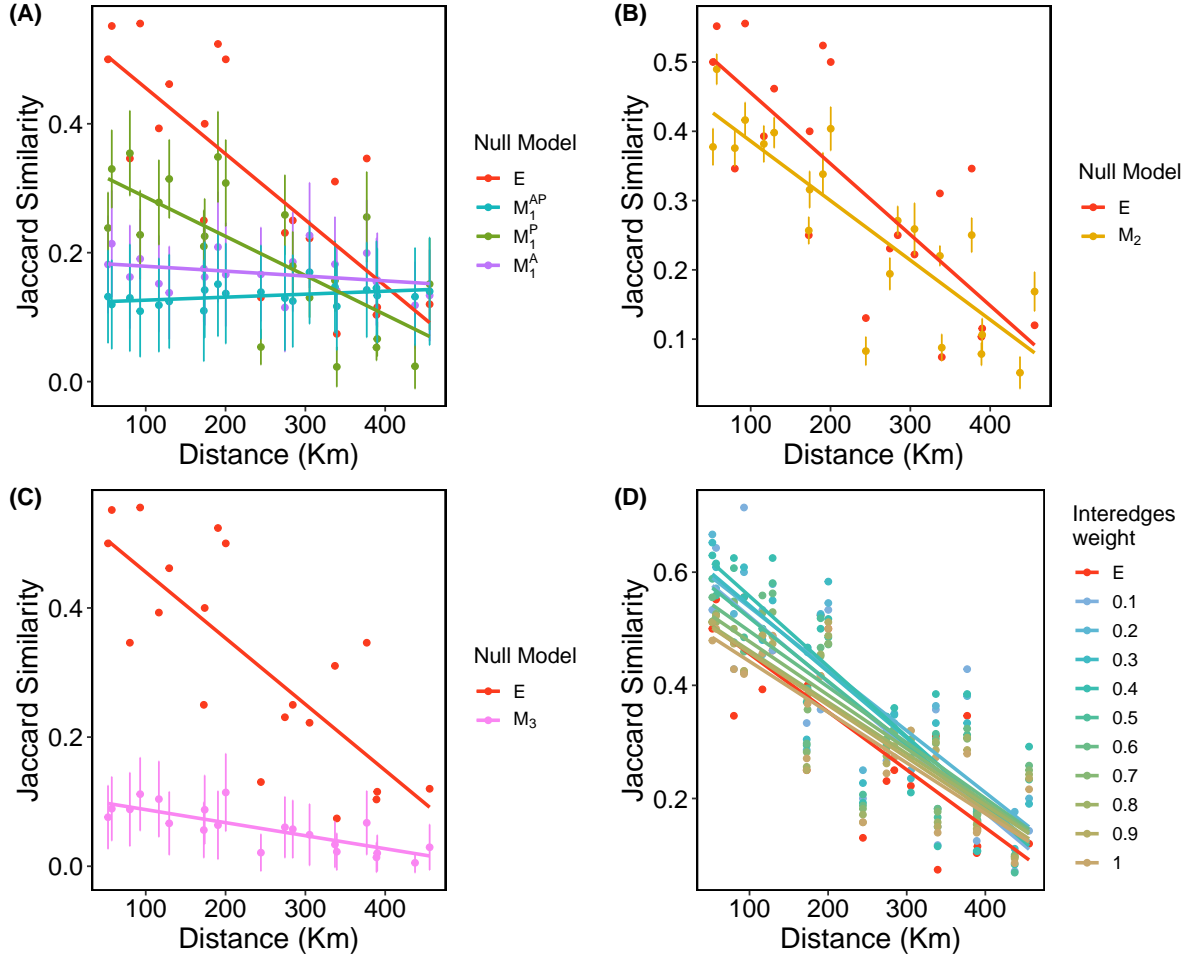


Fig. 3: Drivers of distance decay in structure. The plots show results of linear regression on distance matrices. The response and explanatory variables are similarity in module composition and distance between locations, respectively. The empirical network is depicted with a red line and each null model is depicted by a color (in panels A-C). Each panel represents a different null model. (A) Null model in which plants (M_1^P , green line), pollinators (M_1^A , purple line) or both (M_1^{AP} , light blue line) were shuffled between locations. (B) and (C) null models in which interactions were shuffled between locations (M_2 , yellow line) or within each location (M_3 , pink line), respectively. (D) Null model M_4 , in which the weight of interlayer links were fixed to uniform values. ‘E’ refers to the empirical network. In all panels, data points represent the similarity in module composition (calculated using Jaccard) between a pair of locations at a given distance. In panels A-C, data points of the null models are the mean and standard deviation (error bars) across 1,000 simulations.

H₃ - Local factors: Shuffling interactions within each layer still resulted in distance decay in spatial modularity ($R_{M_3}^2 = 0.622$, $P < 0.001$, pink line in Fig. 3C and Fig. 4C, Table S2). However, the distance decay in structure was approximately 5.5 times weaker than in the empirical network as indicated by the slopes of the regression line (-0.0002 vs. -0.0011, Table S2). In addition, the amount of variation explained by distance between locations was significantly lower compared to the empirical network ($P < 0.005$, Fig. 4C). Therefore, local

factors occurring in each location likely drive distance decay in structure at a regional scale.

H₄ - The extent of partner sharing: Setting the partner similarity of species across locations to a uniform value produced a similar pattern of distance decay in module similarity as in the empirical network. This can be seen by the similar slope in all regression lines in Fig. 3D (see also Table S3). Nevertheless, we make two observations. First, module similarity was more variable in closer locations than in distant ones (the regression lines converged towards long distances). Second, the intercept of the regression lines tended to decrease when interlayer links were stronger. Therefore, for closer islands, communities that were strongly linked shared fewer modules.

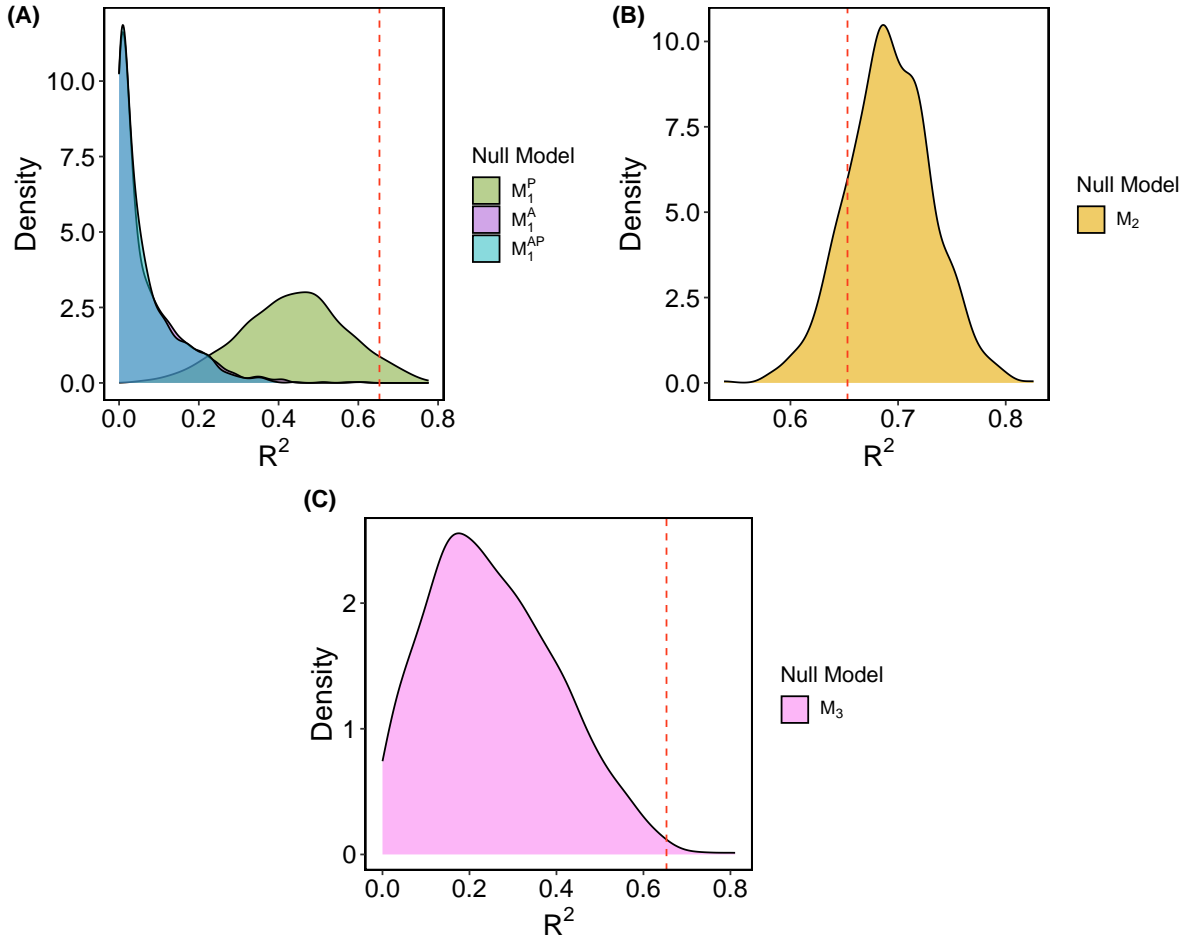


Fig. 4: Comparison of R^2 between the empirical network and null models. Colored density plots represent the distribution of R^2 values resulting from linear regressions on distance matrices, performed on shuffled networks. The R^2 of the empirical network is depicted with the red vertical dashed line. Each panel represents a different type of null model. In (A), plants (M_1^P , green), pollinators (M_1^A , purple) or both species (M_1^{AP} , light blue) were shuffled between locations. In (B) and (C), interactions were shuffled between locations (M_2 , yellow) and within each location (M_3 , pink), respectively.

Discussion

Distance decay is a common pattern in community ecology but distance decay in metacommunity structure, which results from local and regional processes has not been studied. We

provide the first evidence for distance decay in spatial structure, quantifying the importance of local and regional processes underlying it. Our findings offer insights into how metacommunity structure varies across geographical distances at a regional scale. The approach we developed integrates spatial multilayer network analyses and dedicated null models, allowing us to disentangle underlying local and regional processes that drive distance decay in structure. Although several studies have investigated patterns of species distribution across space [6,8,9,16], only a few studies focused on community structure [16], and those that did ignored spatial distributions.

We detected a strong pattern of distance decay in structure, whereby as communities are more distant from each other, their structural similarity tends to decrease. This result is valuable because community structure influences other properties, including stability [13–15]. In particular, a modular structure slows down the spread of perturbations throughout the community, increasing community stability [23,38]. Therefore, quantifying distance decay in structure can be valuable for predicting a spatial response to perturbations that start in a single community and spread, such as invasive species [39], or that affect the entire metacommunity such as changes in temperature. This is particularly crucial for vulnerable ecosystems like islands [40,41].

Species turnover was the main regional process triggering distance decay in structure. This result resonates with previous knowledge because the decrease in species similarity along geographic distances has been recorded globally and for diverse taxa, including plants and pollinator insects [8,9]. Furthermore, evidence suggests that species turnover is the main driver of spatial interaction dissimilarity in pollination networks [9,42] (but see [43]); when two locations share fewer species (and therefore interactions), they are less likely to share modules. Of the species groups, pollinators drove distance decay (null model M_1). This is consistent with previous observations, which showed that distance decay in species composition is stronger for pollinators than plants [6,9].

Species turnover can also be captured with interlayer links, whose number and weight depend on the extent of partner similarity. When artificially tuning the strength of interlayer links, module similarity was more variable in close islands than in distant ones (Fig. 3D). This is because distant islands have only few interlayer links (few species share at least one partner). Therefore, the weight of interlayer links has a minor influence on modularity in distant locations compared to close ones. By increasing the strength of links regardless of space or the number of observed partners, we effectively created links stronger than observed, which should result in more module sharing. Nevertheless, we obtain an opposite pattern for closer islands: communities that were strongly linked in the null model shared fewer modules. This is because of the way the modularity algorithm works. Species that are very strongly linked to themselves between islands will tend to form their own module, reducing module similarity. Because species tend to share fewer partners as geographical distances increase [9], this null model teaches us that the number of partners shared is an important determinant of distance decay in module structure.

Contrary to species turnover, interaction rewiring between locations did not drive distance decay in structure. A plausible explanation is that the high turnover of species in the Canary Islands [9] resulted in limited shared potential partners between locations. Such scenario reduces the chances of a species to interact with a different partner when we shuffle interactions between locations, likely producing a similar structural pattern as in the empirical network. In contrast, Magrath *et al.* [44] found that interaction rewiring is an important mechanism driving interaction dissimilarity through space in continental systems; nevertheless, its effect on the structure was not tested.

Local factors also played an important role in determining distance decay as shown by the strong effect of within-layer interactions on multilayer modularity (null model M_3). These findings may be attributed to the characteristics of the system, primarily composed of volcanic islands. Differences in the geological age and size of the Canary Islands [27] could have led to dissimilar coevolution and speciation processes, resulting in variations in species composition (high endemism) [24,25,27]. In addition, geological age influences habitat heterogeneity (e.g., composition of the plant community). These local differences could, in turn, influence regional processes occurring between islands. For instance, the disparate coevolution of species between islands may explain the observed high relevance of species turnover to structure at regional scale, as opposed to interaction rewiring. Similarly, recent studies also showed that high degree of endemism triggers turnover of species across space and elevation gradients [45,46]. In addition, the large distance between the closest islands (52 km) and the low dispersal ability of plants and insects suggest that dispersal limitation does not play a major role in species turnover between islands in the Canary region.

Our work can be advanced in several ways. *First*, our study focused on inter-island distance decay (insularity effects). Islands comprise particular characteristics (e.g., isolation, size, high endemism) that could result in distinct ecological patterns compared to continental systems. Quantifying distance decay in structure in non-island systems or across gradients should be a straightforward continuation of this work. *Second*, local barriers to connectivity and distance decay within an island could also operate, similarly to the distinction between isolation by distance and isolation by resistance in population genetics [18]. For example, in agroecosystems, habitat fragmentation affects species turnover by altering patch connectivity [47]. The relative effects of distance vs. connectivity on spatial structure in terrestrial systems could be tested using the circuit theory approach [17]. *Third*, understanding spatial effects on community structure is essential because it provides a new dimension to the structure-stability relationship [13–15]. We encourage future studies to investigate how this relationship operates across space, for instance using spatial models of robustness. *Fourth*, community properties emerge from the interplay between different types of ecological interactions [48–50]. Therefore, future studies could improve understanding of biogeographical patterns by considering the spatial distribution of multitrophic communities. *Fifth*, we used multilayer modularity but other properties calculated using inter-layer links can be informative. Moreover, interlayer links can be defined in other ways, encoding other hypotheses.

Altogether, our study provides a general framework for linking communities in space using multilayer networks and for how to test different hypotheses regarding the structure of those networks. The multilayer metacommunity framework we present here and its associated null models can be readily applied to other systems. Our findings highlight the role of species turnover, in particular that of pollinator species, and their local interactions in driving distance decay in structure. This understanding can help in better coping with the consequences of global change.

Acknowledgments

We thank Rohit Sahasrabudde for valuable comments on an early iteration of this research.

Funding statement

SP was supported by the Israel Science Foundation (ISF grant 1281/20) and Human Frontiers Science Program (HFSP award number RGY0064/2022). AV is supported by the Israel Academy of Sciences and Humanities & Council for Higher Education Excellence Fellowship Program for

International Postdoctoral Researchers.

Conflict of interest

The authors declare no conflict of interest

Ethics statement

This article does not present research with ethical considerations.

Data and code availability

Data and code will be available upon acceptance of this preprint.

References

1. Soininen, J. Species Turnover along Abiotic and Biotic Gradients: Patterns in Space Equal Patterns in Time? *Bioscience* **60**, 433–439 (2010).
2. Burkle, L. A. & Alarcón, R. The future of plant-pollinator diversity: understanding interaction networks across time, space, and global change. *Am. J. Bot.* **98**, 528–538 (2011).
3. Tylianakis, J. M. & Morris, R. J. Ecological Networks Across Environmental Gradients. *Annu. Rev. Ecol. Evol. Syst.* **48**, 25–48 (2017).
4. Mittelbach, G. G. & Schemske, D. W. Ecological and evolutionary perspectives on community assembly. *Trends Ecol. Evol.* **30**, 241–247 (2015).
5. Nekola, J. C. & White, P. S. The distance decay of similarity in biogeography and ecology. *J. Biogeogr.* **26**, 867–878 (1999).
6. Soininen, J., McDonald, R. & Hillebrand, H. The distance decay of similarity in ecological communities. *Ecography* **30**, 3–12 (2007).
7. Poisot, T., Canard, E., Mouillot, D., Mouquet, N. & Gravel, D. The dissimilarity of species interaction networks. *Ecol. Lett.* **15**, 1353–1361 (2012).
8. Graco-Roza, C. *et al.* Distance decay 2.0 - A global synthesis of taxonomic and functional turnover in ecological communities. *Glob. Ecol. Biogeogr.* **31**, 1399–1421 (2022).
9. Trøjelsgaard, K., Jordano, P., Carstensen, D. W. & Olesen, J. M. Geographical variation in mutualistic networks: similarity, turnover and partner fidelity. *Proc. Biol. Sci.* **282** (2015).
10. CaraDonna, P. J. *et al.* Interaction rewiring and the rapid turnover of plant-pollinator networks. *Ecol. Lett.* **20**, 385–394 (2017).
11. Dallas, T. A. & Jordano, P. Spatial variation in species' roles in host–helminth networks. *Philos. Trans. R. Soc. Lond. B Biol. Sci.* **376**, 20200361 (2021).
12. Dallas, T. A., Jordano, P. & Blowes, S. Parasite species richness and host range are not spatially conserved. *Glob. Ecol. Biogeogr.* **31**, 663–671 (2022).
13. Carpentier, C., Barabás, G., Spaak, J. W. & De Laender, F. Reinterpreting the relationship between number of species and number of links connects community structure and stability. *Nat Ecol Evol* **5**, 1102–1109 (2021).
14. Thébault, E. & Fontaine, C. Stability of ecological communities and the architecture of mutualistic and trophic networks. *Science* **329**, 853–856 (2010).
15. Tylianakis, J. M., Laliberté, E., Nielsen, A. & Bascompte, J. Conservation of species interaction networks. *Biol. Conserv.* **143**, 2270–2279 (2010).

16. Dallas, T. & Poisot, T. Compositional turnover in host and parasite communities does not change network structure. *Ecography* **41**, 1534–1542 (2018).
17. McRae, B. H., Dickson, B. G., Keitt, T. H. & Shah, V. B. Using circuit theory to model connectivity in ecology, evolution, and conservation. *Ecology* **89**, 2712–2724 (2008).
18. Pérez-Méndez, N., Jordano, P. & Valido, A. Persisting in defaunated landscapes: Reduced plant population connectivity after seed dispersal collapse. *J. Ecol.* **106**, 936–947 (2018).
19. Dehling, D. M. *et al.* Similar composition of functional roles in Andean seed-dispersal networks, despite high species and interaction turnover. *Ecology* **101**, e03028 (2020).
20. Pilosof, S., Porter, M. A., Pascual, M. & Kéfi, S. The multilayer nature of ecological networks. *Nat Ecol Evol* **1**, 101 (2017).
21. Galai, G. *et al.* Scale-dependent signatures of microbial co-occurrence revealed via multi-layer network analysis.
22. Olesen, J. M., Bascompte, J., Dupont, Y. L. & Jordano, P. The modularity of pollination networks. *Proc. Natl. Acad. Sci. U. S. A.* **104**, 19891–19896 (2007).
23. Grilli, J., Rogers, T. & Allesina, S. Modularity and stability in ecological communities. *Nat. Commun.* **7**, 12031 (2016).
24. Dormann, C. F., Fründ, J. & Martin Schaefer, H. Identifying Causes of Patterns in Ecological Networks: Opportunities and Limitations. *Annual review of ecology* (2017).
25. Ponisio, L. C. *et al.* A Network Perspective for Community Assembly. *Frontiers in Ecology and Evolution* **7** (2019).
26. Timóteo, S., Correia, M., Rodríguez-Echeverría, S., Freitas, H. & Heleno, R. Multilayer networks reveal the spatial structure of seed-dispersal interactions across the Great Rift landscapes. *Nat. Commun.* **9**, 140 (2018).
27. Trøjelsgaard, K. *et al.* Island biogeography of mutualistic interaction networks. *J. Biogeogr.* **40**, 2020–2031 (2013).
28. Bascompte, J., Jordano, P. & Olesen, J. M. Asymmetric coevolutionary networks facilitate biodiversity maintenance. *Science* **312**, 431–433 (2006).
29. Shapiro, J. T. *et al.* Multilayer networks of plasmid genetic similarity reveal potential pathways of gene transmission. *ISME J.* **17**, 649–659 (2023).
30. Rosvall, M. & Bergstrom, C. T. Maps of random walks on complex networks reveal community structure. *Proc. Natl. Acad. Sci. U. S. A.* **105**, 1118–1123 (2008).
31. Rosvall, M. & Bergstrom, C. T. Mapping change in large networks. *PLoS One* **5**, e8694 (2010).
32. Farage, C., Edler, D., Eklöf, A., Rosvall, M. & Pilosof, S. Identifying flow modules in ecological networks using Infomap. *Methods Ecol. Evol.* (2021).
33. R Core Team. R: A language and environment for statistical computing. *R foundation for statistical computing Vienna, Austria* (2021).
34. Legendre, P., Lapointe, F.-J. & Casgrain, P. MODELING BRAIN EVOLUTION FROM BEHAVIOR: A PERMUTATIONAL REGRESSION APPROACH. *Evolution* **48**, 1487–1499 (1994).
35. Lichstein, J. W. Multiple regression on distance matrices: a multivariate spatial analysis tool. *Plant Ecol.* **188**, 117–131 (2007).

36. Goslee, S. C. & Urban, D. L. The ecodist Package for Dissimilarity-based Analysis of Ecological Data. *J. Stat. Softw.* **22**, 1–19 (2007).
37. Oksanen, Blanchet, Kindt & others. Community ecology package. *R package* (2013).
38. Stouffer, D. B. & Bascompte, J. Compartmentalization increases food-web persistence. *Proc. Natl. Acad. Sci. U. S. A.* **108**, 3648–3652 (2011).
39. Díaz, S. *et al.* Pervasive human-driven decline of life on Earth points to the need for transformative change. *Science* **366** (2019).
40. Bellard, C., Rysman, J.-F., Leroy, B., Claud, C. & Mace, G. M. A global picture of biological invasion threat on islands. *Nat Ecol Evol* **1**, 1862–1869 (2017).
41. Russell, J. C. & Kueffer, C. Island Biodiversity in the Anthropocene. *Annu. Rev. Environ. Resour.* **44**, 31–60 (2019).
42. Simanonok, M. P. & Burkle, L. A. Partitioning interaction turnover among alpine pollination networks: spatial, temporal, and environmental patterns. *Ecosphere* (2014).
43. Hervías-Parejo, S. *et al.* Spatio-temporal variation in plant–pollinator interactions: a multilayer network approach. *Oikos* **2023** (2023).
44. Magrach, A., Artamendi, M., Lapido, P. D., Parejo, C. & Rubio, E. Indirect interactions between pollinators drive interaction rewiring through space. *Ecosphere* **14** (2023).
45. Costa, F. M. *et al.* Islands in a green ocean: Spatially structured endemism in Amazonian white-sand vegetation. *Biotropica* **52**, 34–45 (2020).
46. Minachilis, K. *et al.* High species turnover and unique plant-pollinator interactions make a hyperdiverse mountain. *J. Anim. Ecol.* **92**, 1001–1015 (2023).
47. Markfeld, M., Rotem, G. & Ziv, Y. A network approach for analyzing arthropod diversity and natural patches prioritization in a fragmented agroecosystem. *Landsc. Ecol.* **37**, 1527–1541 (2022).
48. Vitali, A. *et al.* Invasive species modulate the structure and stability of a multilayer mutualistic network. *Proc. Biol. Sci.* **290**, 20230132 (2023).
49. Montesinos-Navarro, A., Hiraldo, F., Tella, J. L. & Blanco, G. Network structure embracing mutualism–antagonism continuums increases community robustness. *Nature Ecology & Evolution* **1**, 1661–1669 (2017).
50. Sauve, A. M. C., Fontaine, C. & Thébault, E. Structure-stability relationships in networks combining mutualistic and antagonistic interactions. *Oikos* **123**, 378–384 (2014).

Table S1: Location diversity measures. Each location is an island or the mainland (Western Sahara). The last row in the table refers to the union of all other locations. For each location we provide the number of plant (S_{plants}) and pollinator S_{poll} species, the α diversity ($S_{plants} + S_{poll}$), and the number of interactions (L). For the region, we provide the γ diversity.

Location	Scale	S_{plants}	S_{poll}	α diversity	γ diversity	L
Western Sahara	Local	12	60	72	-	541
Fuerte ventura	Local	9	56	65	-	598
Gran Canaria	Local	12	50	62	-	727
Fasnia	Local	16	68	84	-	699
Tenerife	Local	19	59	78	-	1019
Gomera	Local	15	52	67	-	632
Hierro	Local	11	54	65	-	511
Canary Islands	Region	39	248	-	287	4727

Table S2: Output of linear regression models performed to examine structure distance decay in the empirical and null models (M_1, M_2, M_3).

Model	Intercept	Slope	R^2	p - value	df
Empirical	0.568	-0.0011	0.653	<0.001	19
M_1^P	0.346	-0.0006	0.518	<0.01	19
M_1^A	0.186	-0.000075	0.105	0.267	19
M_1^{AP}	0.121	-0.000046	0.169	0.231	19
M_2	0.471	-8.59E-04	0.712	<0.001	19
M_3	0.107	-2.0E-04	0.622	<0.001	19

Table S3: Output of linear regression models performed to examine structure distance decay in the empirical and the null model M_4 .

Model	Weight interlayer link	Intercept	Slope	R^2	p - value	df
Empirical	Empirical	0.568	-0.001	0.653	<0.001	19
M_4	0.1	0.637	-0.0011	0.684	<0.001	19
M_4	0.2	0.647	-0.0010	0.735	<0.001	19
M_4	0.3	0.658	-0.0011	0.725	<0.001	19
M_4	0.4	0.681	-0.0012	0.711	<0.001	19
M_4	0.5	0.631	-0.0011	0.778	<0.001	19
M_4	0.6	0.594	-0.00098	0.741	<0.001	19
M_4	0.7	0.571	-0.00094	0.734	<0.001	19
M_4	0.8	0.552	-0.0009	0.712	<0.001	19
M_4	0.9	0.549	-0.00092	0.71	<0.001	19
M_4	1	0.531	-0.00089	0.715	<0.001	19

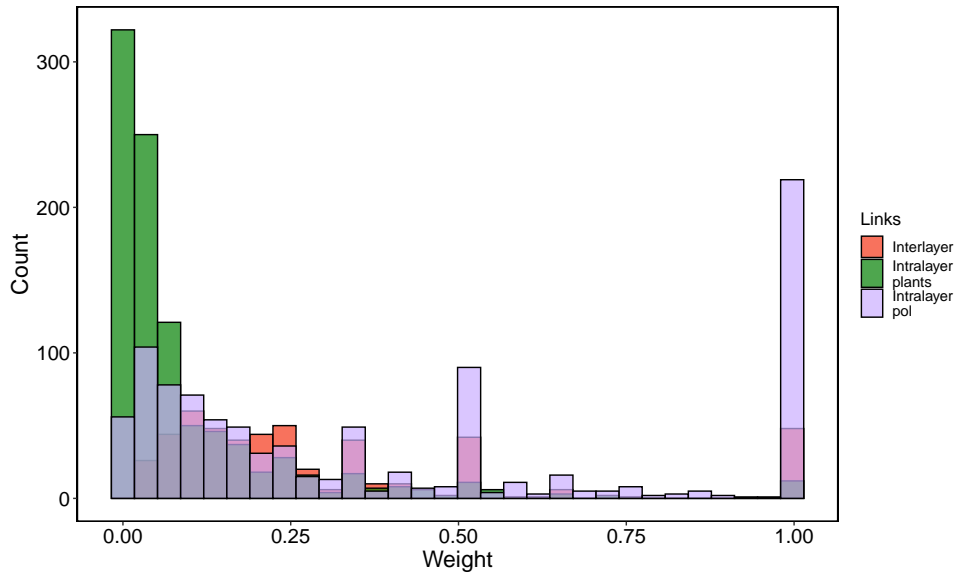


Fig. S1: Distribution of inter and intralayer links. Each bar indicates the frequency of links with a specific value. Color of bars indicates the type of link: red = interlayer link, green = plant-pollinator intralayer link, and light purple = pollinator-plant intralayer link.

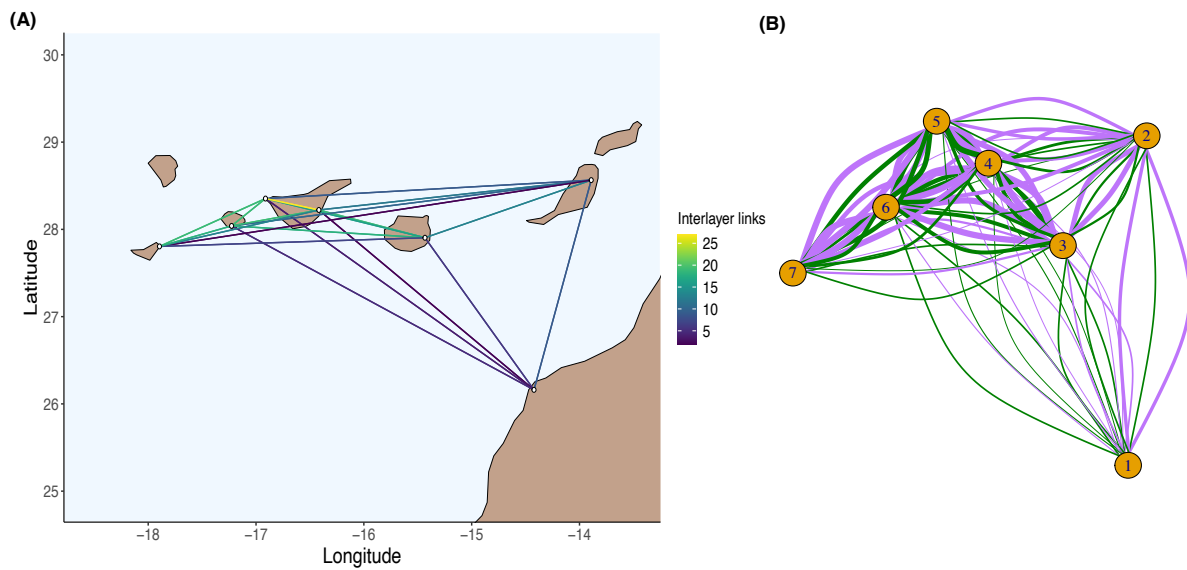


Fig. S2: Distribution of interlayer links across locations. (A) Total number of interlayer links across locations. Each line represents the presence of at least one interlayer link across locations. Color of lines indicates the number of interlayer links. (B) Weight of interlayers links across locations. Each line represents a different interlayer link. Line color indicates the trophic group of species involved: green = plant, purple = pollinator. Width of lines represents the weight. Thicker lines indicate the same species shares a high proportion of partners across locations. Circle numbers correspond to a specific location: 1 = Western Sahara, 2 = Fuerte Ventura, 3 = Gran Canaria, 4 = Fasnía, 5 = Tenerife, 6 = Gomera, 7 = Hierro.

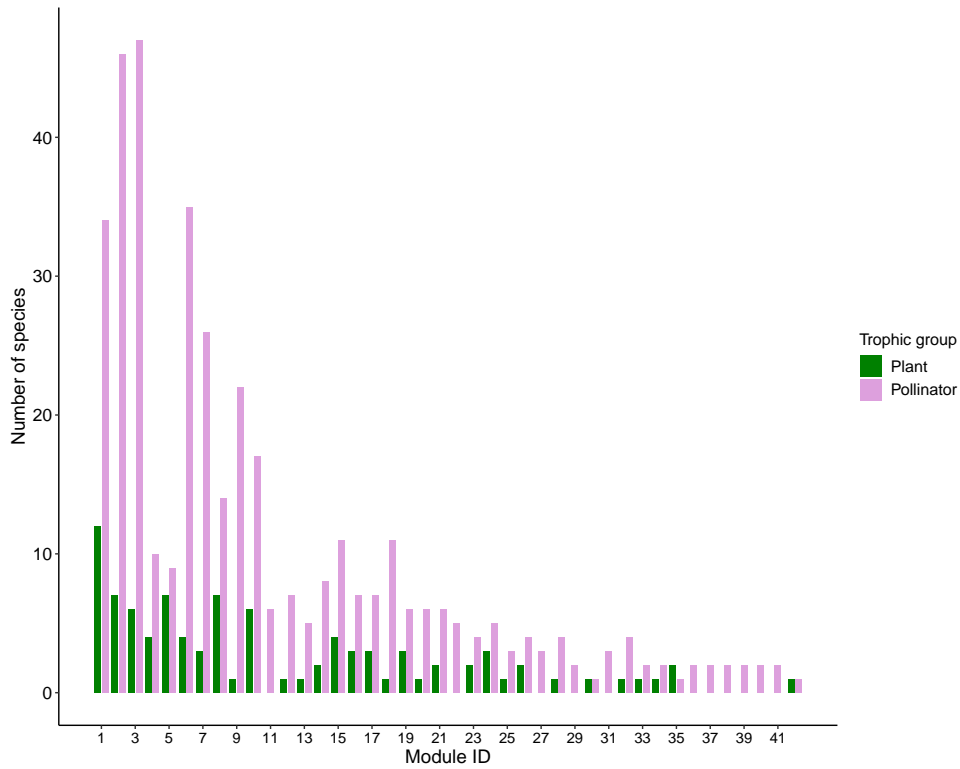


Fig. S3: Number of species in each module. Each bar represents the number of plant (green) and pollinator (purple) species in each module.

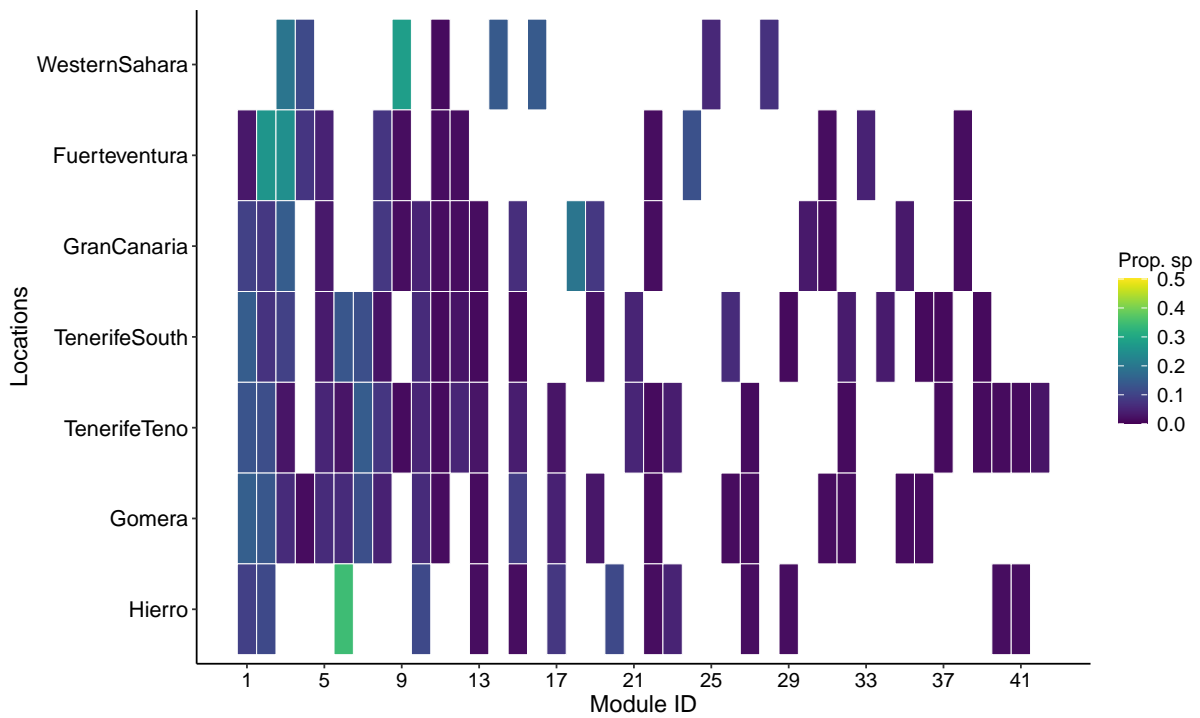


Fig. S4: Proportion of species in each module. Each rectangle represents the presence of a specific module in a location. Color of rectangles indicates the proportion of species of each island that are integrating each module.

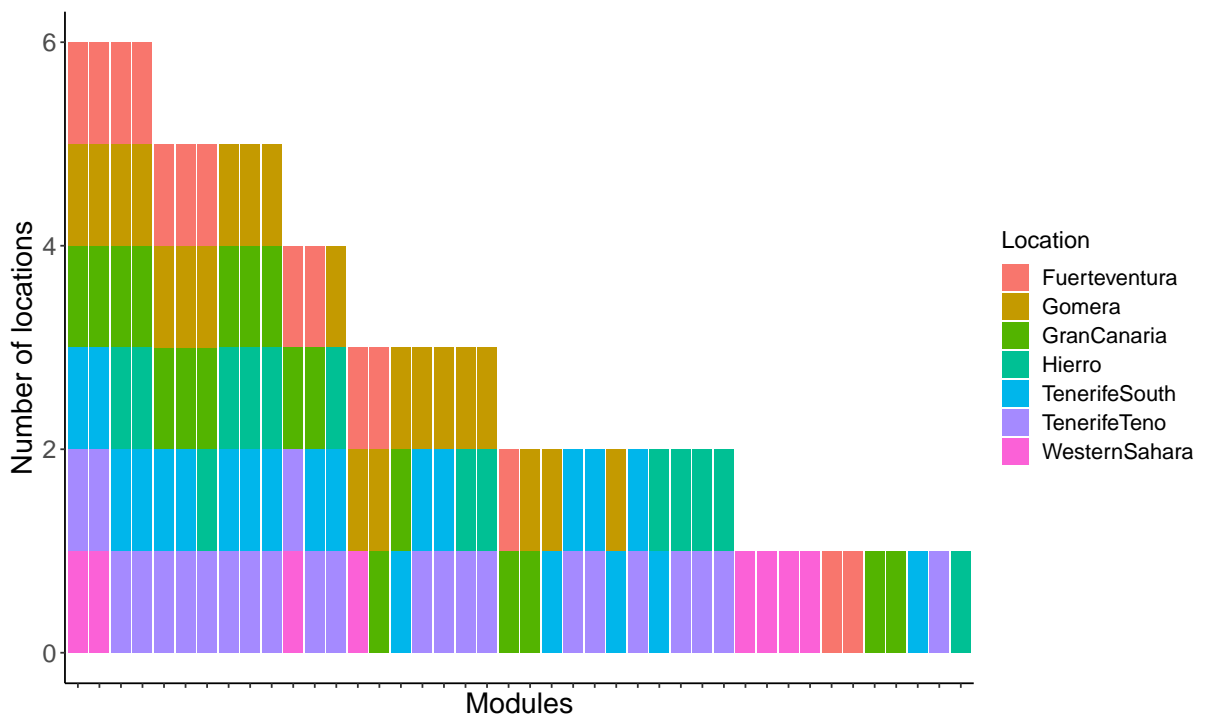


Fig. S5: Distribution of modules across locations. Each bar indicates the number of locations where a specific module was found. In addition, color represents the identity of locations. Modules are ordered from higher to lower number of occurrences across locations (from left to right).